Analysis of a Tumour Growth Model with MATLAB

Keng-Cheng Ang
kengcheng.ang@nie.edu.sg
National Institute of Education
Nanyang Technological University
1, Nanyang Walk, Singapore 637616
Singapore

Abstract

Mathematical modelling can play a very important role in cancer research. In particular, modelling the growth of tumour has the potential of shedding light on the mechanisms of tumour cell growth and proliferation. In this paper, we examine and analyze one such model with the aid of MATLAB.

The model, first proposed by Sherratt and Chaplain in 2001, is based on a set of partial differential equations. The equations describe the growth, movement and death of tumour cells, accompanied by a supply of nutrients. This spatial-temporal model depends on a number of parameter values as well as rate functions. The model is solved numerically using finite difference method implemented on MATLAB. Effects and influence of the parameter values and rate functions are analyzed. Results are validated against a set of known experimental data, and good agreement is observed.

1   Introduction

Cancer, the name given to a group of diseases in which abnormal cells grow and reproduce uncontrollably, is one of the major causes of death in the world (http://www.who.org). In Singapore, cancer ranks as the number one killer and one in three people will die of cancer (http://www.moh.gov.sg). It is, therefore, not surprising that cancer research receives a lot of attention in the scientific world.

Under normal conditions, cells in our body grow, divide, die and replace themselves in an orderly, controlled manner. However, if the process gets out of control, cells can grow too rapidly without any order and develop into a lump which is called a tumour [7]. These tumours can be benign or malignant, and the latter is cancerous. A malignant tumour essentially consists of cancer cells that are able to spread beyond the original site, invade neighbouring tissues, and spread to other parts of the body in a process called metastasis.

The early stages of tumour growth are difficult to be studied clinically as the size of the tumour is too small. However, experiments have been carried out to study early growth of tumour *in vitro*, using the multicellular spheroid approach [10]. In such studies, a seed cell taken from a tumour cell line is placed in a medium containing appropriate nutrients. The

resulting culture grows into a ball of cells (or spheroid), and the cell mass can grow up to several millimetres in diameter.

As the tumour grows, it becomes more difficult for nutrients to reach the core or centre of the spheroid since the outer cells tend to consume these nutrients first. Eventually, cells near the core can become so deficient that they lose their ability to be proliferative and enter the quiescent stage. Quiescent cells are still alive, and can recover with sufficient nutrients [4]. As the tumour grows further, prolonged nutrient deficiency can cause the cells near the core to die, forming a group of dead cells known as a necrotic core. Thus, it is believed that at this stage of tumour growth, three layers of tumour cells are observed: necrotic, quiescent and proliferating cells. This is shown schematically in Figure 1. As depicted, a typical multicell spheroid consists of an outer shell of proliferating cells, an inner layer of quiescent cells which are dormant but viable, and a central core of necrotic material.
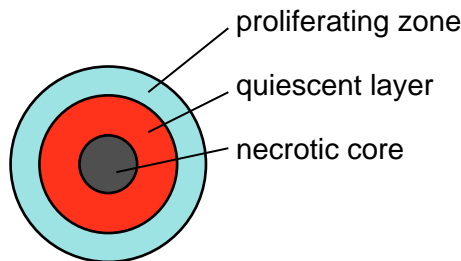

Figure 1: Three-layer structure of a tumour spheroid

Experiments and studies such as the above are useful in shedding light on the growth dynamics of tumour cells. One main experimental observation is that cancer cells need a high nutrient environment to proliferate, while low nutrient levels lead to cell death. In addition, tumour growth is influenced by cell movements as well as other cell growth factors.

The tumour growth described thus far is restricted to the early stage where the tumour has yet to develop its own blood vessels. This is known as the avascular stage, and is the focus of discussion in this paper.

2   Mathematical models of tumour growth

Mathematical modelling of avascular tumours can be seen as the first step in building models for tumour growth in later stages and can play a very important role in cancer research. In particular, modelling the growth of tumour can possibly provide valuable insights into the mechanisms of tumour cell growth and proliferation.

Different approaches, resulting in different types of models, have been used to develop mathematical models of avascular tumour growth. Burton [2] was probably the first to propose that diffusion and nutrient concentration limit the growth of solid tumour growth. Since then, numerous models based on spatio-temporal interactions between tumour cell populations and nutrients have been suggested. An example of these early models is in the influential work by Greenspan [6]. In addition to limited nutrient supply and production of growth inhibitors, Greenspan's model assumes that the disintegration of dead cells in the necrotic core further regulate the tumour size.

Another model suggested by Adam [1] assumes that the self-inhibitory effect can be explained by non-uniform production of the growth inhibitors. Ward and King [12] considered a tumour spheroid in terms of a continuum of live and dead cells, and showed that the tumour will grow exponentially at first, and then levelling off to a linear growth.

Sherratt and Chaplain [9] formulated a model in terms of cell densities of proliferating, quiescent and necrotic cells in a one-dimensional domain in space. Cell movement is incorporated in the model, which is essentially based on a simple competitive model. More recently, Tan and Ang [11] modified the model to include random variation in cellular and extracellular processes. This model succeeds in providing a more realistic description of avascular tumour growth and is a reasonably good attempt at modelling complex biological tumour growth processes through the use of random terms in the model equations.

The model chosen for further analysis in this paper is the Sherratt-Chaplain model and its variants as proposed by Tan and Ang.

2.1   The Model

In this model, the cell densities for the proliferating, quiescent and necrotic cells are denoted by $p(x, t)$, $q(x, t)$ and $n(x, t)$ respectively, where t represents time and x is the spatial coordinate. Necrotic cells are dead and hence non-motile, while proliferating and quiescent cells can move. However, in a close-packed environment such as a tumour spheroid, movement of cells can be restricted. This phenomenon, known as contact inhibition of migration, is incorporated into the model by assuming that the overall viable cell flux is given by $\frac{\partial}{\partial x}(p + q)$. Moreover, if we assume that the two cell populations have equal motility, then the movement terms of the proliferating and quiescent cells will be given as

$$\frac{\partial}{\partial x}\left(\frac{p}{p+q}\frac{\partial(p+q)}{\partial x}\right) \text{ and } \frac{\partial}{\partial x}\left(\frac{q}{p+q}\frac{\partial(p+q)}{\partial x}\right)$$

respectively.

Suppose proliferating cells grow at a rate that is limited by crowding of the total cell population, and that they become quiescent at a rate that depends on the concentration $c(x, t)$ of some nutrients. Suppose quiescent cells become necrotic also at a rate that depends on $c(x, t)$. Then, we can write down the following set of model equations.

$$\frac{dp}{dt} = \frac{\partial}{\partial x}\left(\frac{p}{p+q}\frac{\partial(p+q)}{\partial x}\right) + g(c)\,p(1 - p - q - n) - f(c)\,p \tag{1}$$

$$\frac{dq}{dt} = \frac{\partial}{\partial x}\left(\frac{q}{p+q}\frac{\partial(p+q)}{\partial x}\right) + f(c)\,p - h(c)\,q \tag{2}$$

$$\frac{\partial n}{\partial t} = h(c)\,q \tag{3}$$

Note that in this set of model equations, the value of 1 corresponds to a completely close-packed population. Also, $g(0)$ is set to 1 to provide a suitable initial condition. Also, the functions f and h are decreasing functions, with both tending to zero as c tends to $+\infty$, while g is an increasing function. Since the rate of cells becoming quiescent is normally higher than

the rate of cells entering necrosis, we expect $f(c) > h(c)$. Given these conditions, one can specify suitable or appropriate functional forms for f, g and h.

As for nutrient concentration, we use the form suggested by [9]. That is,

$$c = \frac{c_0 \gamma}{\gamma + p} \left(1 - \alpha \left(p + q + n\right)\right) , \tag{4}$$

where α and γ are dimensionless parameters.

The system of equations (1) to (4) may be solved numerically using the finite difference formulations for the equations. Using forward differencing for time and central differencing for space, we obtain the following set of finite difference equations.

$$p_i^{j+1} = p_i^j + \Delta t \left[u_i^j + g(c_i^j) \, p_i^j \left(1 - p_i^j - q_i^j - n_i^j\right) - f(c_i^j) \, p_i^j\right] \tag{5}$$

$$q_i^{j+1} = q_i^j + \Delta t \left[v_i^j + f(c_i^j) \, p_i^j - h(c_i^j) \, q_i^j\right] \tag{6}$$

$$n_i^{j+1} = n_i^j + \Delta t \left[h(c_i^j) \, q_i^j\right] \tag{7}$$

$$c_i^j = \frac{\gamma}{\gamma + p_i^j} \left[1 - \alpha \left(p_i^j + q_i^j + n_i^j\right)\right] \tag{8}$$

where

$$u_i^j = \frac{(p_{i+1}^j - p_{i-1}^j) r_i^j (r_{i+1}^j - r_{i-1}^j) + 4 \, p_i^j \, r_i^j \, (r_{i+1}^j - 2r_i^j + r_{i-1}^j) - p_i^j \, (r_{i+1}^j - r_{i-1}^j)^2}{4 \, (\Delta x)^2 \, (r_i^j)^2} \tag{9}$$

$$v_i^j = \frac{(q_{i+1}^j - q_{i-1}^j) r_i^j (r_{i+1}^j - r_{i-1}^j) + 4 \, q_i^j \, r_i^j \, (r_{i+1}^j - 2r_i^j + r_{i-1}^j) - q_i^j \, (r_{i+1}^j - r_{i-1}^j)^2}{4 \, (\Delta x)^2 \, (r_i^j)^2} \tag{10}$$

$$r_i^j = p_i^j + q_i^j \tag{11}$$

In the above finite difference equations, Δt and Δx refer to the time steps and space intervals respectively, and the superscript for the dependent variables indicate the time level and space position respectively. For instance, p_i^j would refer to the density of the proliferating cells at the jth time level and i^{th} space position.

The finite difference scheme given by equations (5) to (11) can be implemented on MATLAB to provide a platform for analyzing the model itself. However, several parameters need to be set, and functional forms of f, g and h must be given. In addition, one has to decide what kind of output is desired.

The program list in Appendix A is one possible implementation with $\alpha = 0.9$ and $\gamma = 10$. These parameter values are chosen arbitrarily, and can be changed if so desired for further analysis. Three sets of graphs showing the distribution of proliferating, quiescent and necrotic cells at different times are generated in this program. These will be discussed in detail in Section 3.

2.2   Functional forms, initial and boundary conditions

The model (and hence the program) requires the functions $f(c)$, $g(c)$ and $h(c)$ to be defined. In this discussion, we choose $f(c) = (1 - \tanh(4c - 2))/2$ and $h(c) = f(c)/2$, as in [9]. For $g(c)$, in contrast to the linear form chosen by Sherratt and Chaplain, a more appropriate Gompertz growth rate is used. That is, we set $g(c) = \beta e^{\beta c}$ with $\beta = 0.5$. These functions are written in MATLAB as shown below.

```
function y = f(c)
y=0.5*(1-tanh(4*c-2));

function y=h(c)
y=0.5*f(c);

function y=g(c)
global beta
y=beta*exp(beta*c);
%y=1+0.2*c;
```

In addition to the above functions, we need to specify the initial conditions and boundary conditions. We shall assume that at $t = 0$, $q(x,0) = 0$, $n(x,0) = 0$, $c = 1$, and the proliferating cell density decreases exponentially as x increases. Thus, we let $p(x,0) = e^{0.1x}$. As for the boundary conditions, it is usual to assume zero-flux at the boundaries. That is,

$$\frac{\partial p}{\partial x} = 0 \text{ and } \frac{\partial q}{\partial x} = 0 \text{ at } x = 0 \text{ and as } x \to \infty.$$

In terms of implementation, it is not possible to let $x \to \infty$. We therefore need to choose a value of x that is sufficiently large. After experimenting with various values, it is found that $x = 210$ is appropriate and good enough to observe patterns of the evolution of cell densities.

2.3   Model Calibration

One way to analyze this model further is to compare its results with experimental data. To do so, we first need to calibrate the model to the data set. In this discussion, the data chosen are the experimental results from Nirmala et al [8]. Graphs of the data and results obtained from the calibrated model are shown in Figure 2.
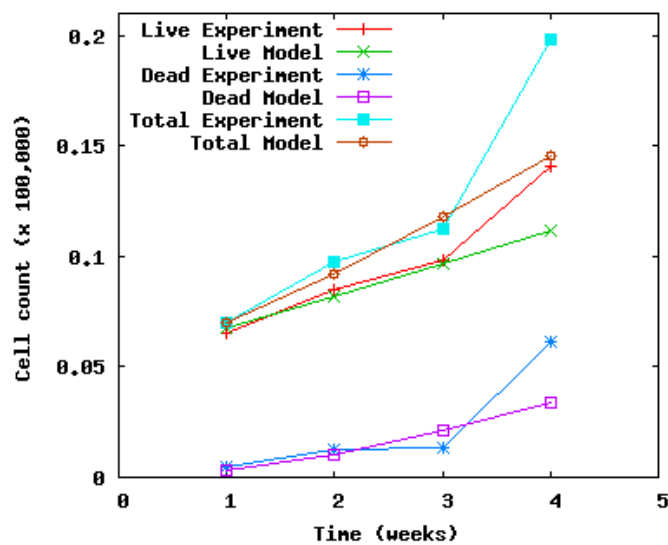

Figure 2: Comparison of cell counts between calibrated model and data from [8]

The model is calibrated by choosing an appropriate scaling factor to transform cell densities to match the cell counts in the experimental data. The reference point in this calibration is chosen to be $t = 1$, at which time the experimental total cell count is about 7015. The total cell density from the model is around 15.809; hence a scaling factor of about 443.7249 is used. With this value, the total live cells (that is, proliferating and quiescent) and dead cells (necrotic) as predicted by the model can be compared against the experimental data. As can be observed in Figure 2, the model produces results which compare quite well with the experimental data.

3 Results and Discussion

3.1 Graphical results

The calibrated model is solved for the set of functional forms of f, g and h, and initial and boundary values as described earlier. Parameters values may be varied to observe and analyze their effects on the model results. Due to space constraints, only one set of results (with $\alpha = 0.8$, $\beta = 0.5$ and $\gamma = 10$ is presented as graphs as shown in Figure 3.
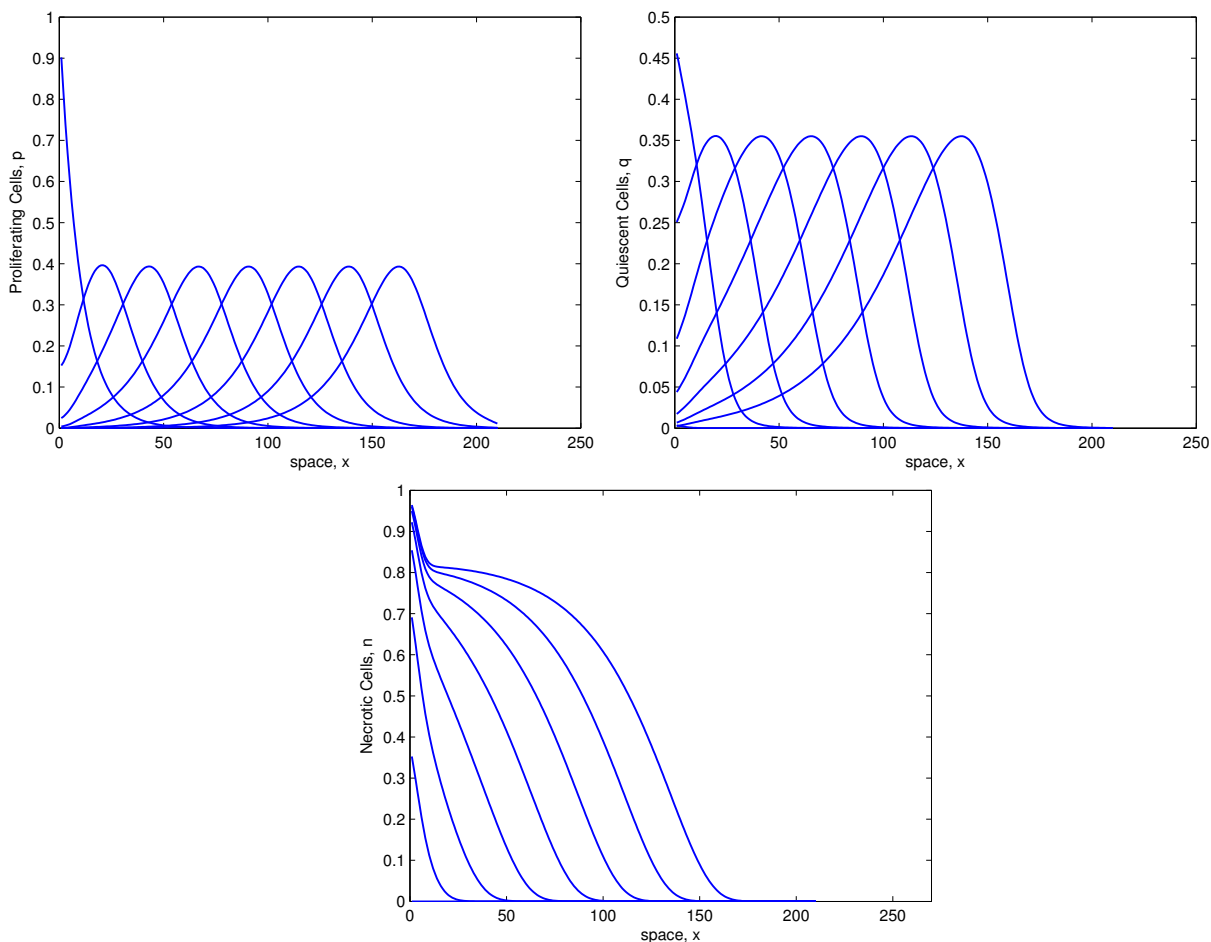

Figure 3: Numerical solutions with $\alpha = 0.8$, $\beta = 0.5$ and $\gamma = 10$. Cell densities of proliferating, quiescent and necrotic cells plotted as a function of space at times $t = 0, 2, \ldots, 14$. Curves move from left to right as time increases.

From Figure 3, it is observed that an advancing pulse of proliferating cells is accompanied by a corresponding band of quiescent cells as time increases. The necrotic cells seem to be concentrated at the core initially ($t = 2$ to $t = 8$). As time passes, the necrotic cells continue to develop at the core, but begin to disperse towards the outer edge of the tumour spheroid.

Although necrotic cells are building up with time, no tumour regression is detected. This is expected as the model does not restrict or limit nutrient flow sufficiently, and no therapy or control measure is introduced. These results compare well with experimental findings in [8]. Both the current model and the experiment results report no limiting spheroid volume.

The graphical output presented in Figure 3 shows the differences in the evolution of the tumour sub-populations of proliferating, quiescent and necrotic cells. Apart from nutrient supply and the inherent differences in their growth dynamics, other factors such as cell stress and growth inhibiting factors could play a role in influencing the model results. One could further analyze the model by varying the nutrient coefficient α. In fact, if a smaller value of α is chosen (such as $\alpha = 0.4$) to represent increased access to nutrients, we observe a higher and quicker build-up of live tumour cells over a longer span of time.

3.2   Visualizing Tumour Growth

Although the model is one-dimensional in space, by assuming radial symmetry, one can construct an image of the cell distribution in two or three dimensions at any time t. At a particular time t, the distribution of a cell type over the x space dimension is obtained from the model. For this distribution, at any point $x = r$, one could distribute the cells around the circle with radius r.

As an example, consider the number of proliferating cells at time $t = T$ and at position $x = r$, which would be given by $p(r, T)$. We distribute the these cells along the circumference of the circle with radius r. This may be done by randomly picking a number θ between 0 and 2π (to represent an angle from a reference line) and plotting a marker on this circumference at the point (r, θ) in polar coordinates. This is done for the whole range of values of x and at various time intervals to construct a sequence of images showing how the tumour evolves over time. A series of snapshots of tumour images generated in this manner is shown in Figure 4.
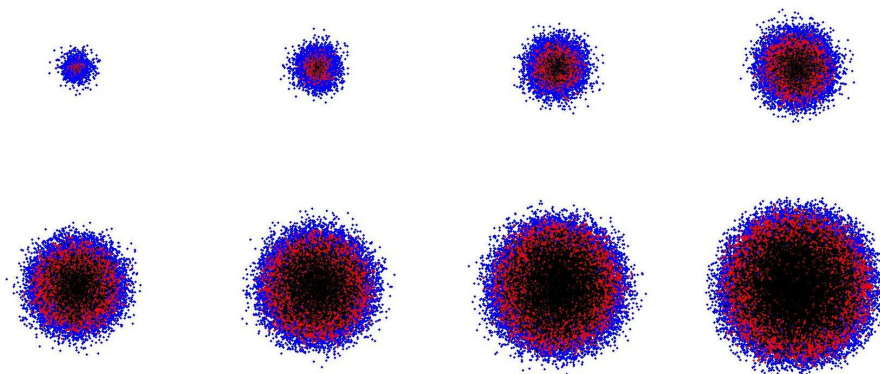

Figure 4: Snapshots of simulated tumour growth at $t = 2, 4, \ldots, 16$ units, with blue, red and black coloured dots representing proliferating, quiescent and necrotic cells respectively

The images shown in Figure 4 are saved to files using the MATLAB statement (with a systematic way of naming the output files),

```
print('-djpeg','-r100',sprintf('%s_%s',prefix,num2str(Nm)));
```

These can then be pieced together to provide an animation of tumour growth. The MATLAB program segment is listed in Appendix B. This segment is to be appended to the main program listed in Appendix A to construct the images, and produce a short movie clip or animation of the tumour growth process for better visualization.

As can be seen in Figure 4, the tumour starts with a high concentration of proliferating cells and relatively small concentration of quiescent and necrotic cells. This gradually changes as t increases and the tumour is seen to be growing fast. When t increases to 8 and beyond, a clear necrotic core begins to form. The quiescent region begins to thicken while the proliferating layer becomes thin. These observations in the model are consistent with experimental results reported by Dorie et al [3] and Folkman and Hochberg [5].

4   Conclusion

In this paper, we discuss a slightly modified model for an avascular tumour growth, originally proposed by Sherratt and Chaplain. The model is solved using a finite difference scheme, and implemented on MATLAB. Calibration of the model is done using experimental data obtained from Nirmala. Results are presented in the form of graphs and as a series of tumour images for better visualization.

Quantitatively, the model had produced results which compare fairly well with the experimental results reported by Nirmala. More importantly, this model provides qualitative results which can be further analyzed and studied.

The use of MATLAB in this discussion illustrates the important role of technology in research in mathematical modelling. Not only does MATLAB help in providing a computing platform for implementing the numerical scheme efficiently, it also serves as a useful tool for generating visual images resulting from the model.

Acknowledgement

References

[1] Adam, J. A., "A simplified mathematical model of tumour growth", *Mathematical Bioscience*, 1986, **81**, 224-229.

[2] Burton, A. C., "Rate of growth of solid tumours as a problem of diffusion", *Growth*, 1966, **30**, 157-176.

[3] Dorie, M., Kcallman, R. and Coyne, M., "Effect of cytochalasin b, nocodazole and iradiation on migration and internalization of cells and microspheres in tumour cell spheroids", *Experimental Cell Research*, 1986, **166**, 370-378.

[4] Freyer, J. P. and Schor, P. L., "Regrowth of cells from multicell tumour spheroids", *Cell and Tissue Kinetics*, 1987, **20**, 249.

[5] Folkman, J. and Hochberg, M., "Self-regulation of growth in three dimensions", *Journal of Experimental Medicine*, 1973, **138**, 745-753.

[6] Greenspan, H. P., "Models for the growth of a solid tumour by diffusion", *Studies in Applied Mathematics*, 1972, **52**, 317-340.

[7] Melicow, M. M., "The three-steps to cancer: A new concept of carcinogenesis", *Journal of Theoretical Biology*, 1982, **94**, 471-511.

[8] Nirmala, C., Rao, J. A., Ruifrok, A. C., Langford, L. A. and Obeyesekere, M., "Growth characteristics of glioblastoma spheroids", *International Journal of Oncology*, 2001, **19**, 1109-1115.

[9] Sherratt, J. A. and Chaplain, M. A. J., "A new mathematical model for avascular tumour growth", *Journal of Mathematical Biology*, 2001, **43**, 291-312.

[10] Sutherland, R. M., "Cell and environment interaction in tumour microregions: the multi-cell spheroid model", *Science*, 1988, **240**, 177-184.

[11] Tan, L. S. and Ang, K. C., "A numerical simulation of avascular tumour growth", *ANZIAM Journal*, 2005, **46(E)**, C902-C917.

[12] Ward, J. P. and King, J. R., "Mathematical modelling of avascular tumour growth", *IMA Journal of Mathematics Applied in Medicine & Biology*, 1997, **14**, 39-69.

Appendix A: Listing of main MATLAB program

```
%% main program for tumour growth
clear; clc;
global alpha beta gamma
% set parameter values
alpha = 0.9; beta = 0.5; gamma = 10;
dx = 1; X = 210; dt = 0.004; T = 16;
c0 = 1;
% set up arrays
x  = [dx:dx:X]; Nx = round(X/dx); Nt = round(T/dt);
p = zeros(1,Nx); nextp = zeros(1,Nx);
q = zeros(1,Nx); nextq = zeros(1,Nx);
n = zeros(1,Nx); nextn = zeros(1,Nx);
u = zeros(1,Nx); v = zeros(1,Nx); r = zeros(1,Nx); c = zeros(1,Nx);
P = zeros(Nt,Nx); Q = zeros(Nt,Nx); N = zeros(Nt,Nx);
% set initial values
p = exp(-0.1.*x);
% start FDM time-stepping
for k=1:Nt
```

```
   r = p + q;
   c = (c0.*gamma./(gamma+p)).*(1-alpha.*(p+q+n));
   for i=2:Nx-1
       u(i)=((p(i+1)-p(i-1))*r(i)*(r(i+1)-r(i-1))+ ...
           4*p(i)*r(i)*(r(i+1)-2*r(i)+r(i-1))- ...
           p(i)*(r(i+1)-r(i-1))^2)/(2*(dx*r(i))^2);
       v(i)=((q(i+1)-q(i-1))*r(i)*(r(i+1)-r(i-1))+ ...
           4*q(i)*r(i)*(r(i+1)-2*r(i)+r(i-1))- ...
           q(i)*(r(i+1)-r(i-1))^2)/(2*(dx*r(i))^2);
   end
   nextp=p+dt.*(u+g(c).*p.*(1-(p+q+n))-f(c).*p);
   nextq=q+dt.*(v+f(c).*p-h(c).*q);
   nextn=n+dt.*(h(c).*q);
   p=nextp;
   q=nextq;
   n=nextn;
   P(k,:)=p; Q(k,:)=q; N(k,:)=n;
end
figure(1)
for n=1:500:Nt
    plot(P(n,:),'LineWidth',1.2); hold on;
end
axis([0 270 0 0.6]);
figure(2)
for n=1:500:Nt
    plot(Q(n,:),'LineWidth',1.2); hold on;
end
axis([0 270 0 0.6]);
figure(3)
for n=1:500:Nt
    plot(N(n,:),'LineWidth',1.2); hold on;
end
axis([0 270 0 1]);
```

Appendix B: Listing of program segment on constructing animation

```
% create images for cells
rand('state', sum(100*clock));
prefix='t';
Nm=0;
figure(1)
for n=1:250:Nt
    Nm=Nm+1;
    for i=1:Nx
        tP=round(P(n,i)); tQ=round(Q(n,i)); tN=round(N(n,i));
        for m=1:tP
```

```matlab
            theta=2*pi*rand();
            plot(i*sin(theta),i*cos(theta),'b.'); hold on;
        end
        for m=1:tQ
            theta=2*pi*rand();
            plot(i*sin(theta),i*cos(theta),'r.'); hold on;
        end
        for m=1:tN
            theta=2*pi*rand();
            plot(i*sin(theta),i*cos(theta),'k.'); hold on;
        end
        axis square
        axis([-300 300 -300 300])
    end
    print('-djpeg','-r100',sprintf('%s_%s',prefix,num2str(Nm)));
end

clear MM
for i=1:Nm
    [XX,map]=imread(sprintf('%s_%s',prefix,num2str(i)),'jpeg');
    imagesc(XX);
    MM(i)=getframe;
    pause(0.1);
end
```